

## Long-range odd triplet order parameter with equal spin pairing in diffusive Co/In contacts

B. Almog,<sup>\*</sup> S. Hacoheh-Gourgy, A. Tsukernik, and G. Deutscher

Tel Aviv University, P. O. Box 39040, Tel Aviv 69978 Israel

(Received 15 November 2009; published 30 December 2009)

We have measured the conductance of single, double, and multiple junction superconductor (S)/ferromagnet (F) devices made of Co and In. The contacts are created by pinholes in the CoO which prevent the local destruction of superconductivity. The conductance of the single junction has a V-shape cusp at zero bias typical of a nodal order parameter such as  $p$  wave. In the double S/F device the nonlocal conductance at low energies is positive and larger in the parallel state than in the antiparallel state by 30%. The same effect was found in multiple S/F junctions in parallel. The results can be explained by an odd triplet order parameter inside S, up to a distance of 150 nm from the S/F interface.

DOI: [10.1103/PhysRevB.80.220512](https://doi.org/10.1103/PhysRevB.80.220512)

PACS number(s): 74.45.+c, 74.20.Rp, 74.50.+r, 74.78.Na

The physics of the interface between a superconductor (S) and a ferromagnet (F) has attracted much interest in recent years. While the effect of an exchange field on the critical temperature of F/S/F sandwiches has been known for some time,<sup>1</sup> nonlocal effects due to crossed Andreev-Saint James (ASJ) reflections and cotunneling in devices where two (or more) nearby F branches are attached to a common S bar have been predicted<sup>2,3</sup> and observed in some circumstances.<sup>4-6</sup> Additionally, it was predicted that, under certain conditions, such as spin scattering<sup>7</sup> or inhomogeneous magnetization,<sup>8</sup> Cooper pairs near an S/F interface will have an odd triplet order parameter (OP) with equal spin pairing. A long-range proximity effect into F has indeed been observed, consistent with a triplet OP.<sup>9,10</sup> However, there is still no direct experimental evidence for the existence of a triplet state inside S, for the expected  $p$ -wave symmetry of the order parameter in that state, as well as for its long-range character.

In this Rapid Communication we present measurements of diffusive single- and multiple-terminal S/F devices of Co and In, where the contact between Co and In is mostly through pinholes in a thin CoO at the interface. We show that the conductance of single S/F junctions is governed by ASJ reflections with a V-shaped cusp around zero bias, which is evidence for a nodal OP in accordance with theoretical predictions of a  $p$ -wave symmetry of the order parameter in a triplet state at S/F interfaces. In the three-terminal Co/In/Co device we find that the nonlocal conductance is energy independent below the local superconducting energy gap and is lower by 30% at small bias for antiparallel (AP) Co magnetizations than for parallel (P) ones. We also show that the resistance of several Co/In junctions connected in parallel is higher in the antiparallel magnetization state. These experiments on double-terminal and multiterminal devices indicate that the triplet state generated at our S/F interfaces extends in S up to distances of at least 100 nm.

We fabricated structures consisting of single, double, and multiple S/F contacts by means of  $e$ -beam lithography in a two-step process. Cobalt bars 30 nm thick were evaporated first using  $e$ -gun evaporation technique at  $10^{-8}$  Torr. In the second *ex situ* step, a 60-nm-thick In bar, crossing over the Co legs, was evaporated using a thermal source with the substrate cooled to liquid nitrogen temperature. The short mean free path  $l \sim 40$  nm, evaluated by the ratio between

room- and low-temperature resistivities, reduces the superconducting coherence length down to  $\xi_s \sim 115$  nm (dirty limit). In the double- and multiple-terminal devices two types of Co legs with different aspect ratios,  $300 \text{ nm} \times 6 \text{ } \mu\text{m}$  and  $200 \text{ nm} \times 12 \text{ } \mu\text{m}$ , were chosen to obtain different coercive fields in order to allow us to control their magnetization separately. The distance between the Co stripes was 150 nm in the double configuration and 100 nm in the multiconfiguration device, both on the order of  $\xi_s$ .

One of the problems with transparent S/F junctions is the destruction of superconductivity due to the large exchange field in the ferromagnet, which tends to align the spins of the electrons and thus to destroy Cooper pairs. However, if the contact size is small enough (less than  $\xi_s$ ) this effect can be avoided almost completely. It was shown<sup>11</sup> that by letting the ferromagnetic metal oxidize for a few hours, one gets junctions with weak, if any, proximity effect that behaves as good point-contact junctions in a planar geometry due to the presence of pinholes in the oxide layer. While in a previous publication we used Ni, here we chose Co because Co nanowires behave as single domains in the longitudinal direction with a very sharp transition.<sup>12</sup> This is crucial for multiterminal devices in order to produce legs with distinct parallel and antiparallel magnetic states. The differential conductance measurements were conducted using a Keithley's current source (6221) and a nanovoltmeter (2182A) combination.

Figure 1 shows the striking similarity between the differential resistance of one of our single Co/In junctions and that of a point contact on a single crystal of  $\text{Sr}_2\text{RuO}_4$ . Both show a similar cusp at zero bias. Such cusps are a well-known feature of contacts with a superconductor having order parameter nodes, such as the high- $T_c$  cuprates.<sup>13</sup> The cusps seen on  $\text{Sr}_2\text{RuO}_4$  as well as on our S/F contacts are in accordance with the theoretical prediction that the  $dI/dV$  characteristics of a point contact with a superconductor having a  $p$ -wave symmetry order parameter has a finite slope at zero bias when the surface is perpendicular to an antinodal direction.<sup>14</sup> The temperature dependence of the zero-bias resistance  $[R(T)]$  of another single S/F junction is shown in Fig. 2(B). The transition temperature is 4 K, which is typical of thin In film. A resistance peak due to charge imbalance (CI) appears at  $T_c$  because of the cross geometry.<sup>11</sup> Below  $T_c$  the resistance drops, reaching a minimum at 3.1 K and thereafter increasing constantly. The bias dependence of the differential

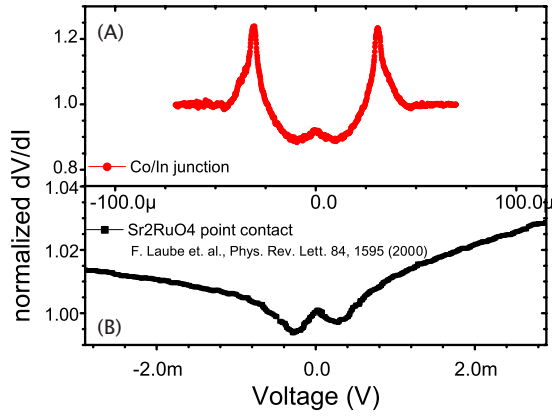


FIG. 1. (Color online) (A) The normalized differential resistance ( $dV/dI$ ) of a single Co/In junction. The cusp at zero bias is a fingerprint of a nodal order parameter. (B) A point-contact measurement of  $\text{Sr}_2\text{RuO}_4$ , which is a  $p$ -wave superconductor.

conductance at different temperatures is shown in Fig. 2(A). Its main features are an enhancement of the differential conductance (up to  $\sim 23\%$ ) at moderate energies and a cusp at zero bias. At higher energies the conductance is reduced until a critical voltage is reached, where the critical current in the In film on top of the Co is exceeded and the normal state conductance is restored. The S/F contact is rather transparent as evident by the low contact resistance ( $10^{-8} \Omega \text{ cm}^2$ ) and the sharp decrease in  $R(T)$  below  $T_c$ , confirming its point-contact nature. V-shaped cusps were observed in six out of seven junctions measured.

We now turn to describe the local and nonlocal conductances of the double junction device. For the nonlocal con-

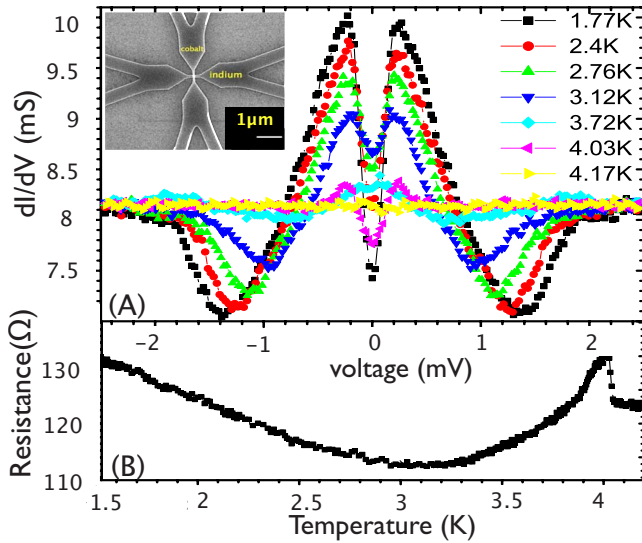


FIG. 2. (Color online) (A) The differential conductance of a single Co/In junction at different temperatures. The conductance is governed by ASJ reflections with a V-shaped cusp at zero bias, which is typical of a nodal order parameter such as  $p$  wave. (B) The resistance as function of temperature. The low contact resistance ( $10^{-8} \Omega \text{ cm}^2$ ) and the sharp decrease in  $R(T)$  below  $T_c$  confirm its point-contact nature. The inset shows a scanning electron microscopy image of the junction.

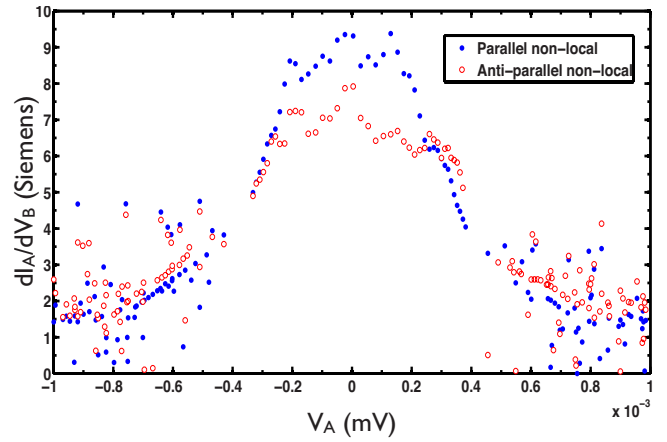


FIG. 3. (Color online) The nonlocal conductance vs local bias  $V_A$ . The decrease in the nonlocal conductance starts when the local bias exceeds the energy gap of In at the contact due to charge imbalance. At low bias the nonlocal conductance in the parallel state is 30% larger than the antiparallel state.

ductance measurement we drive a current through one junction and measure the voltage induced on the other one as illustrated in the inset of Fig. 4. Figure 3 shows the nonlocal,  $(dI_A/dV_B)(V_A)$ , differential conductance as a function of the local bias, measured in the P and AP configurations of the Co legs, at zero field. The respective coercive fields were determined separately by magnetoresistance measurements. The nonlocal conductance is positive and much bigger than the local conductance (a few millisiemens). It is energy independent around zero bias and decreases sharply beyond a certain voltage. Figure 3 shows a distinct difference of about 30% between the nonlocal conductance in the AP and P states at low bias, with the larger one being that in the P state. This is a long-range effect since in this experiment the distance between the Co legs is of 150 nm. We show in the following

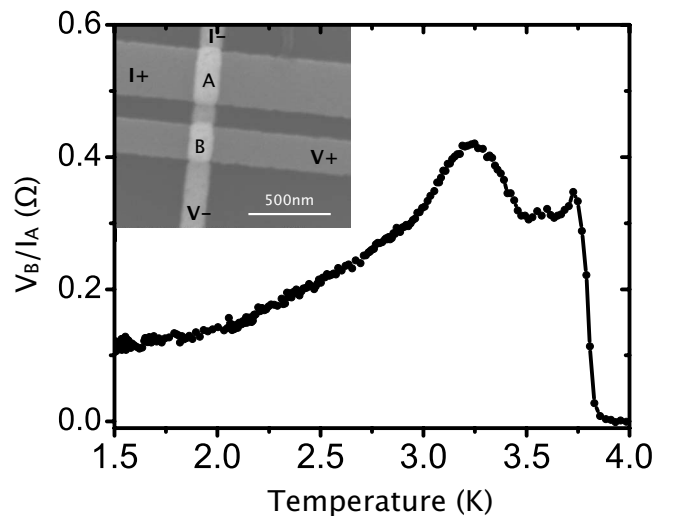


FIG. 4. The nonlocal resistance vs temperature. Resistance shows a maximum at 3.25 K,  $T_c$  of the In at the contact. The nonlocal voltage increases toward  $T_c$  due to the divergence of the charge imbalance length. At low temperatures the nonlocal resistance becomes temperature independent.

discussion that this larger nonlocal conductance in the P state is compatible with the triplet generated at the S/F contacts.

The nonlocal conductances of both P and AP states decreases when the energy of the injected electrons exceeds the local energy gap of In,  $\epsilon \sim 235 \mu\text{V}$ . This is due to the excitation of quasiparticles in the junction, which in turn produce a nonlocal voltage due to CI. Since charge imbalance occurs both at high energies and close to  $T_c$ , where the energy gap is reduced, we expect to see an increase in the nonlocal resistivity when we go closer to the critical temperature as well. Figure 4 shows the zero-bias nonlocal resistance vs temperature. As we get closer to  $T_c$  the nonlocal voltage increases, reaching a maximum at 3.25 K, which is slightly lower than  $T_c$  of the In film. The CI length,<sup>15</sup> over which quasiparticles from normal (N) metal convert into Cooper pairs, diverges close to  $T_c$ ,

$$\Lambda_{Q^*} = \sqrt{D\tau_{Q^*}}, \quad \tau_{Q^*} = \frac{4K_B T}{\pi\Delta(T)} \tau_{in}. \quad (1)$$

Here,  $D$  is the diffusion coefficient,  $\tau_{Q^*}$  is the charge imbalance relaxation time, and  $\Delta(T)$  is the temperature-dependent energy gap. At low temperatures the CI contribution vanishes and the nonlocal resistance becomes temperature independent. In the limit of  $T \rightarrow 0$ , Golubev *et al.*<sup>16</sup> found that for a N/S/N device the nonlocal resistance obeys a universal behavior remarkably independent of both the barrier strength and the normal-metal parameters,

$$R_{nl}(0) = (r_{\xi_s}/2) e^{-|x_2-x_1|/\xi_s}. \quad (2)$$

Here,  $r_{\xi_s}$  is the normal-state resistance of the superconductor wire of length  $\xi_s$  and  $|x_2-x_1|$  is the distance between the two junctions. In our case  $\xi_s \sim 115 \text{ nm}$ ,  $|x_2-x_1| = 150 \text{ nm}$ , and  $r_{\xi_s} \sim 0.45 \Omega$  which give  $R_{nl}(0) = 0.06 \Omega$ . We measure  $R_{nl}(0) \leq 0.1 \Omega$ , in good agreement with theory.

It is instructive at this point to examine the measured quantities. We adopt the notation used by G. Falci *et al.*<sup>17</sup> to describe the local and nonlocal contributions to the current. Taking into account that we impose a zero current in the second junction ( $I_B=0$ ), we get

$$\frac{dI_A}{dV_A} = \frac{(G_{22})(G_{11}) - G_{12}^2}{G_{22}}, \quad \frac{dI_A}{dV_B} = \frac{(G_{22})(G_{11}) - G_{12}^2}{G_{12}}, \quad (3)$$

where  $G_{ii} \equiv G_i + G_{EC} + G_{CA}$  (with  $i=1,2$ ) and  $G_{12} \equiv G_{EC} - G_{CA}$  are the local and nonlocal conductances of the device and  $G_{EC}, G_{CA}$  are the conductances due to elastic cotunneling (EC) and crossed ASJ (CA) reflections, respectively. The differential conductance measurements show that  $dI_A/dV_A \ll dI_A/dV_B$ , which confirms that the single junction conductance is dominant in our junctions,  $G_{22}, G_{11} \gg G_{12}$ . The positive sign indicates that the EC contribution dominates over that of CA.

Since the nonlocal conductance of the P state is 30% larger than the AP state, and keeping in mind that the measured quantity is proportional to  $1/G_{12}$ , we conclude that  $G_{12}^{par} < G_{12}^{APar}$ . This result contradicts the idea that crossed ASJ reflections are favored in the AP state of a double F/S/F structure.<sup>2</sup> We find the opposite to be true—in the AP state the difference between  $G_{EC}$  and  $G_{CA}$  becomes larger.

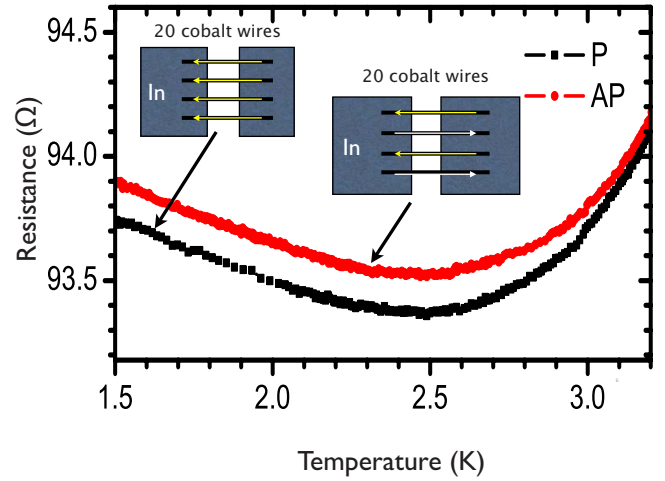


FIG. 5. (Color online) The resistance vs temperature of 20 Co/In junctions connected in parallel. The distance between the Co legs was 100 nm and the distance between the In bars was 1  $\mu\text{m}$ . The resistance of the device in the parallel (see figure) state was lower than that in the antiparallel state only below  $T_c$ .

The same effect was also observed in a different geometry where we measured the resistance of 20 In/Co/In junctions connected in parallel. The distance between the Co legs was 100 nm and the distance between the In bars was 1  $\mu\text{m}$ . The Co legs were set either in a P state or an alternating AP state as illustrated in Fig. 5. As in the double junction device, the resistance in the P state was lower than the AP state. No change was seen above  $T_c$ . The experiments on both double and multiple devices show a correlation between individual S/F junctions on a length scale of 100–150 nm.

The larger conductance in the P state can be understood if the Co/In contacts generate an equal spin triplet state having a  $p$ -wave OP symmetry in the In bar that extends up to distances on the order of the coherence length. This is because in the P state the triplet solution will remain as the preferred one in the F/S/F device if the distance between the F legs is shorter than or on the order of the coherence length, as it is in our experiment, and if—as expected theoretically—the triplet state extends in S up to a distance on the order of the coherence length from the S/F contact. In the extreme case of a fully polarized metal, local ASJ reflections would occur at the individual S/F contacts. On the other hand, the nonlocal processes (CA and EC) would cancel out; much like they do in the case of two normal metals in contact with a singlet superconductor,<sup>17</sup> and there would be no nonlocal voltage. In the case of AP polarizations the triplet state would no longer be favorable due to the opposite exchange fields. The nonlocal mechanisms, EC and CA, would not cancel each other anymore, leading to a finite nonlocal voltage. The polarization of Co is  $\sim 40\%$ , which means that there will be a nonlocal voltage in both states, but it should be lower in the P state than in the AP state as observed. CoO between Co and In in our junctions might play a substantial role in the creation of the triplet. It was predicted theoretically that a spin active layer can lead to the creation of a triplet with equal spin pairing;<sup>7</sup> CoO is antiferromagnetic and might serve as a spin scatterer. It is also possible that mag-

netic inhomogeneities at the interface due to the antiferromagnetic CoO are the key for creating the triplet pairing.<sup>8</sup>

It is important to note that in previously reported measurements of the nonlocal conductance<sup>4,6</sup> no well-defined energy range where the nonlocal conductance is constant was identified. Our unique fabrication technique, in which pinholes in the oxide produce point-contact junctions,<sup>11</sup> allowed us to avoid the strong proximity effect that usually takes place at highly transparent S/F interfaces. Such a strong proximity effect would have drastically reduced the energy gap at the interface which would enable quasiparticle excitation at low energies leading to strong charge imbalance effects already at low bias. The individual characterization of each junction that we have performed establishes that, at energies lower than the local energy gap, charge imbalance plays no important role, as expected. Only then can the non-local processes, CE and CA, be studied.

In conclusion, we fabricated and measured single, double, and multiple Co/In junction devices. The contacts were created by pinholes in the Co oxide, which produced good point-contact junctions with a weak proximity effect. The

conductance of the single Co/In junctions showed ASJ reflections with a V-shaped cusp around zero bias, which is a fingerprint of a nodal order parameter. The nonlocal conductance of a double Co/In device at low bias, where charge imbalance is negligible, was sensitive to the relative magnetization of the cobalt bars. It was higher in the parallel than in the antiparallel state by 30%. We also found that the conductance of multiple Co/In junctions connected in parallel was higher in the parallel state than in the antiparallel configuration. These results clearly show a correlation between neighboring junctions over a distance of 100–150 nm inside S. They are consistent with a triplet order parameter with equal spin pairing at the S/F interface extending inside S up to distances on the order of the coherence length. The V-shaped cusp in the low-bias conductance of single Co/In junctions is consistent with the *p*-wave symmetry order parameter expected of the triplet state.

This work was supported in part by the Israel National Science Foundation (Grant No. 481/07).

\*boazal@post.tau.ac.il

- <sup>1</sup>G. Deutscher and F. Meunier, Phys. Rev. Lett. **22**, 395 (1969).
- <sup>2</sup>G. Deutscher and D. Feinberg, Appl. Phys. Lett. **76**, 487 (2000).
- <sup>3</sup>J. M. Byers and M. E. Flatté, Phys. Rev. Lett. **74**, 306 (1995).
- <sup>4</sup>D. Beckmann, H. B. Weber, and H. v. Löhneysen, Phys. Rev. Lett. **93**, 197003 (2004).
- <sup>5</sup>S. Russo, M. Kroug, T. M. Klapwijk, and A. F. Morpurgo, Phys. Rev. Lett. **95**, 027002 (2005).
- <sup>6</sup>P. Cadden-Zimansky, Z. Jiang, and V. Chandrasekhar, New J. Phys. **9**, 116 (2007).
- <sup>7</sup>A. Kadigrobov, R. I. Shekhter, and M. Jonson, EPL **54**, 394 (2001).
- <sup>8</sup>F. S. Bergeret, A. F. Volkov, and K. B. Efetov, Rev. Mod. Phys. **77**, 1321 (2005).
- <sup>9</sup>V. T. Petrashov, I. A. Sosnin, I. Cox, A. Parsons, and C. Troadec, Phys. Rev. Lett. **83**, 3281 (1999).

- <sup>10</sup>R. S. Keizer, S. T. B. Goennenwein, T. M. Klapwijk, G. Miao, G. Xiao, and A. Gupta, Nature (London) **439**, 825 (2006).
- <sup>11</sup>S. Hacohen-Gourgy, B. Almqvist, and G. Deutscher, Appl. Phys. Lett. **92**, 152502 (2008).
- <sup>12</sup>G. Dumpich, T. P. Krome, and B. Hausmann, J. Magn. Magn. Mater. **248**, 241 (2002).
- <sup>13</sup>A. Kohen, G. Leibovitch, and G. Deutscher, Phys. Rev. Lett. **90**, 207005 (2003).
- <sup>14</sup>M. Yamashiro, Y. Tanaka, and S. Kashiwaya, Phys. Rev. B **56**, 7847 (1997).
- <sup>15</sup>G. E. Blonder, M. Tinkham, and T. M. Klapwijk, Phys. Rev. B **25**, 4515 (1982).
- <sup>16</sup>D. S. Golubev, M. S. Kalenkov, and A. D. Zaikin, Phys. Rev. Lett. **103**, 067006 (2009).
- <sup>17</sup>G. Falci, D. Feinberg, and F. W. J. Hekking, EPL **54**, 255 (2001).